Increased stomach-brain coupling indexes a dimensional signature of negative mental health symptoms

Leah Banellis PhD*[1], Ignacio Rebollo PhD*[2], Niia Nikolova PhD[1], Micah Allen PhD[1,3]

*equal contribution

1. Center of Functionally Integrative Neuroscience, Aarhus University, Denmark.
2. Department of Decision Neuroscience and Nutrition, German Institute of Human Nutrition, Germany.
3. Cambridge Psychiatry, University of Cambridge, United Kingdom.

Corresponding Author: Leah Banellis, leahbanellis@cfin.au.dk.

Short title: The Stomach Brain-Axis in Mental Health

Keywords: brain-body interactions, stomach-brain, mental health, resting fMRI, electrogastrography.

Abstract

Visceral rhythms orchestrate the physiological states underlying human emotion. Chronic aberrations in these brain-body interactions are implicated in a broad spectrum of mental health disorders. However, the specific contributions of the gastric-brain coupling to affective symptoms remain poorly understood. We investigated the relationship between this novel interoceptive axis and mental health symptoms in 243 participants, using a cross validated machine learning approach. We find that frontal parietal brain coupling to the gastric rhythm indexes a dimensional signature of mental health spanning anxiety, depression, stress, and well-being. Control analyses confirm the specificity of these interactions to the gastric-brain axis. Our study establishes coupling between the stomach and brain as a factor in the pathology of mental health, and offers new targets for interventions remediating aberrant brain-body coupling.

Main

Far from being a mere brain in a vat, the nervous system is embedded within an intricate web of visceral rhythms. While philosophy has long championed the embodiment of mind and life[1], it is only more recently that the importance of the visceral body in contextualising brain function has gained widespread recognition[2,3]. In particular, interoceptive processes linking brain and body are thought to be critically important in mood and emotion[2,4], and their larger role in affective symptoms has become a topic of intense interest in mental health research[5].

Research investigating these links have so far focused almost exclusively on the cardiac[6,7], lower gastrointestinal[8,9], and respiratory axes[10–12]. Recent landmark findings demonstrate that, for example, fear conditioning relies on ascending cardiac information[6], and that respiratory rhythms modify neural patterns during emotional processing[13]. Simultaneously, the burgeoning study of gut-brain interaction has produced a plethora of new findings linking the function and biology of the lower gastrointestinal tract or gut to physical and mental health[14–16]. While these and many other findings herald an visceral turn in our understanding of the biology of the mind and its disorder, one particular domain of brain-body coupling remains notably understudied: the upper gastrointestinal tract comprising interconnections between the brain and stomach.

Gastric-brain interactions have recently emerged as a novel frontier in interoception research[17–22]. Hormones secreted by the stomach directly regulate hypothalamic mechanisms that govern satiety and hunger[23]. Additionally, the stomach generates its own independent myoelectrical rhythm, in which the interstitial cells of Cajal pace muscular contractions approximately once every 20 seconds[24]. Previously relegated to merely driving mechanical food digestion, recent discoveries indicate that the gastric rhythm is closely linked to ongoing brain activity through reciprocal vagal innervation[25,26]. This link can be directly modulated through techniques such as non-invasive vagal nerve stimulation[27], bilateral vagotomy in rodent models[28], as well as through emerging pharmacological methods[22,29,30], offering a promising means by which to intervene upon the stomach-brain axis.

Despite the close linkage of emotion and brain-body interaction, it is unclear if alterations in the gastric axis are also consequential for mental health. This gap is curious in part because folk psychology has long centred the stomach as a locus of stress and anxiety: difficult decisions are described as evoking "gut feelings" which in extreme cases, can make one "sick to their stomach."

Conversely, intense moments of love or joy are described as giving "butterflies in the stomach." Aligning with these descriptions, recent empirical findings confirm that subjective disgust, fear, and anxiety are predominantly localised in the stomach[31], and that pharmacological modulation of the gastric rhythm alters emotional processing[22]. On this basis, we hypothesised that inter-individual patterns in gastric-brain coupling might expose unique patterns of affective symptoms, in particular those relating to core mood disorders such as anxiety and depression.

To test this hypothesis, we conducted a large scale neuroimaging study of simultaneous electrogastrographic (EGG) and functional MRI (fMRI) brain imaging in 243 participants. To assess a broad spectrum of mental health symptoms, we employed a multidimensional approach to quantify individual symptom profiles spanning a range of affective and psychiatric disorders. Utilising a multivariate, cross-validated machine learning technique, we estimated highly robust, sensitive, and specific signatures that interrelate these profiles to individual patterns of stomach-brain coupling. Our findings demonstrate that the stomach-brain axis exposes a unique positive-to-negative mode of mental health, revealing a previously unknown target for future clinical intervention research.

Results

Psychiatric functional correlates

To characterise variation in the gastric-brain axis, we utilised simultaneous electrogastrographic (EGG) and resting state fMRI recordings. Following an extensive data quality control procedure (*Methods)*, we estimated stomach-brain coupling for each participant using the phase locking value (PLV) of the EGG and resting state fMRI time series across 209 parcellated whole-brain regions[32] (see Figure 1 for example).

To characterise symptom profiles, we conducted a comprehensive assessment of mental health across 37 self-reported symptom scores encompassing autism, ADHD, empathy, insomnia, interoception, depression, fatigue, social support, somatic symptoms, stress, social anxiety, trait anxiety, well-being, and quality of life (see Supplementary Table 1 for a full list of instruments and subscales). This approach successfully captured robust inter-individual variability spanning a variety of symptom dimensions (see Figure 1). Symptom variance spanned from completely healthy individuals to those experiencing significant distress, such that 30% of the sample exhibited mild depression symptoms, 19% exhibited clinically significant levels of ADHD, 19% medium or more severe

somatic symptoms, 18% trait anxiety, 9% moderate depression symptoms, 7% autism spectrum symptoms, and 5% insomnia (see Supplementary Table 1 for all percentage cut-offs).

Finally, to determine latent patterns interlinking these symptom profiles to stomach-brain coupling, we conducted cross-validated Canonical Correlation Analysis (CCA) (see Figure 1).

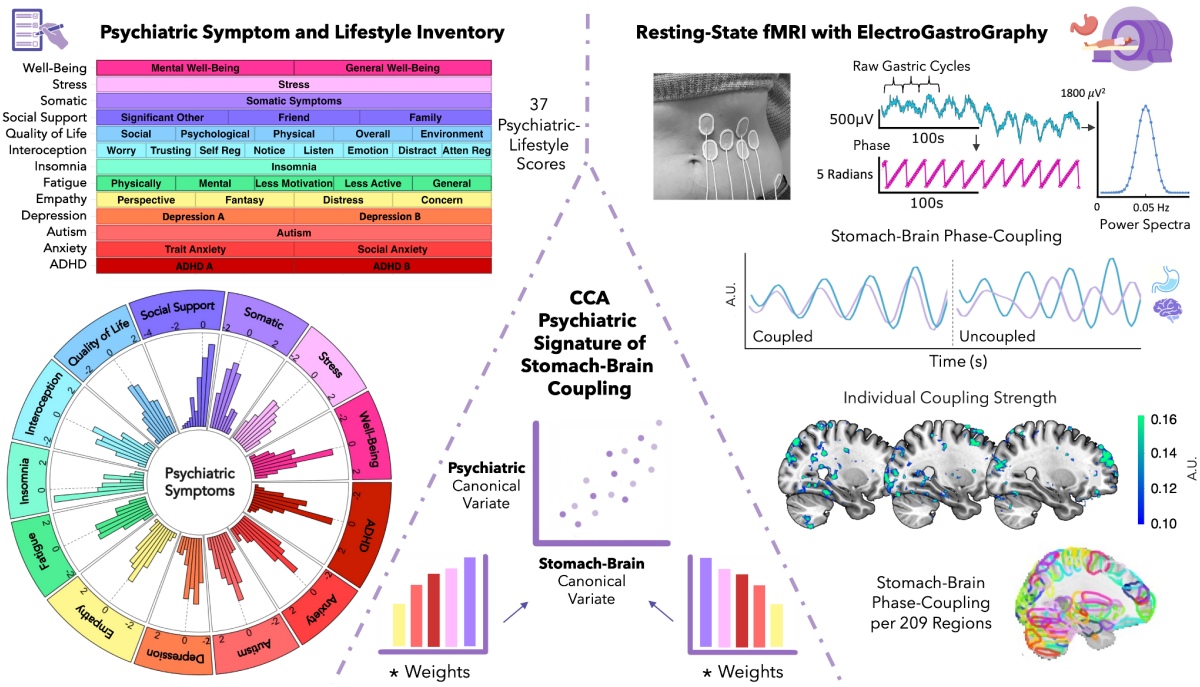

***Figure 1*: Canonical Correlation Analysis of stomach-brain coupling and psychiatric symptoms.**

Figure 1 synthesises the process and outcomes of correlating stomach-brain phase coupling with psychiatric symptoms, as quantified by 37 variables from 16 validated surveys. The top left quadrant presents these variables organised into their respective mental health categories (categorised for visualisation only, the CCA incorporated 37 individual scores), and their distribution is visualised as histograms on the bottom left, reflecting the range of participant profiles. Electrogastrography (EGG) data depicted on the top right demonstrates the extraction of gastric cycle frequency from raw EGG signals, power spectra, and their phase information, essential for identifying stomach-brain coupling. The middle right figure illustrates coupled versus uncoupled states in stomach-brain interaction, with the individual variability in coupling strength highlighted across three brain images from individual participants (plotted on a standard mni152 brain template using MRIcroGL: visualised MNI coordinates plotted: 28, -19, 26, thresholded at 0.1, and small clusters <1000mm^3 removed). For the CCA, stomach-brain phase-coupling is parcellated over 209 brain regions identified using the DiFuMo atlas, shown on the bottom right. The CCA model, depicted centrally, outputs a stomach-brain signature correlating with psychiatric symptoms. This pattern is

represented by canonical variates, which are weighted combinations of the multidimensional psychiatric and stomach-brain coupling data (illustrated as the central scatter plot). These weights, depicted as bar graphs, capture the most significant relationships between gastric-brain coupling and psychiatric profiles.

We observed a significant latent dimension in which stomach-brain coupling was associated with overall mental health (canonical variate in-sample $r(118) = 0.886$, out-sample $r(77) = 0.323$, $p = 0.001$). This was reflected behaviourally as high negative loadings for trait anxiety (STAI trait subscale: -0.827), depression (PHQ9: -0.800, and MDI: -0.782), stress (PSS: -0.773), and fatigue (MFI general fatigue subscale: -0.734), as well as high positive loadings for well-being, and quality of life (highest loadings: WEMWBS: 0.856, WHOQOL psychological subscale: 0.847, WHO: 0.776). The top stomach-brain coupling canonical loadings were found in the left superior angular gyrus (-0.317), right intermediate primus of Jensen (right supramarginal gyrus posterior division using the Harvard-Oxford Cortical Structural Atlas) (-0.284), left inferior precentral sulcus (-0.270), left posterior superior frontal gyrus (-0.269), and left posterior intraparietal sulcus (-0.245). These loadings constitute a pattern of stomach-brain coupling in which more positive symptoms (i.e., improved well-being) are associated with reduced gastric coupling to fronto-parietal brain activity (see Figure 2 and Supplementary Table 3), or conversely, in which more negative symptoms (i.e., increased anxiety, depression, and fatigue) are associated with increased coupling.

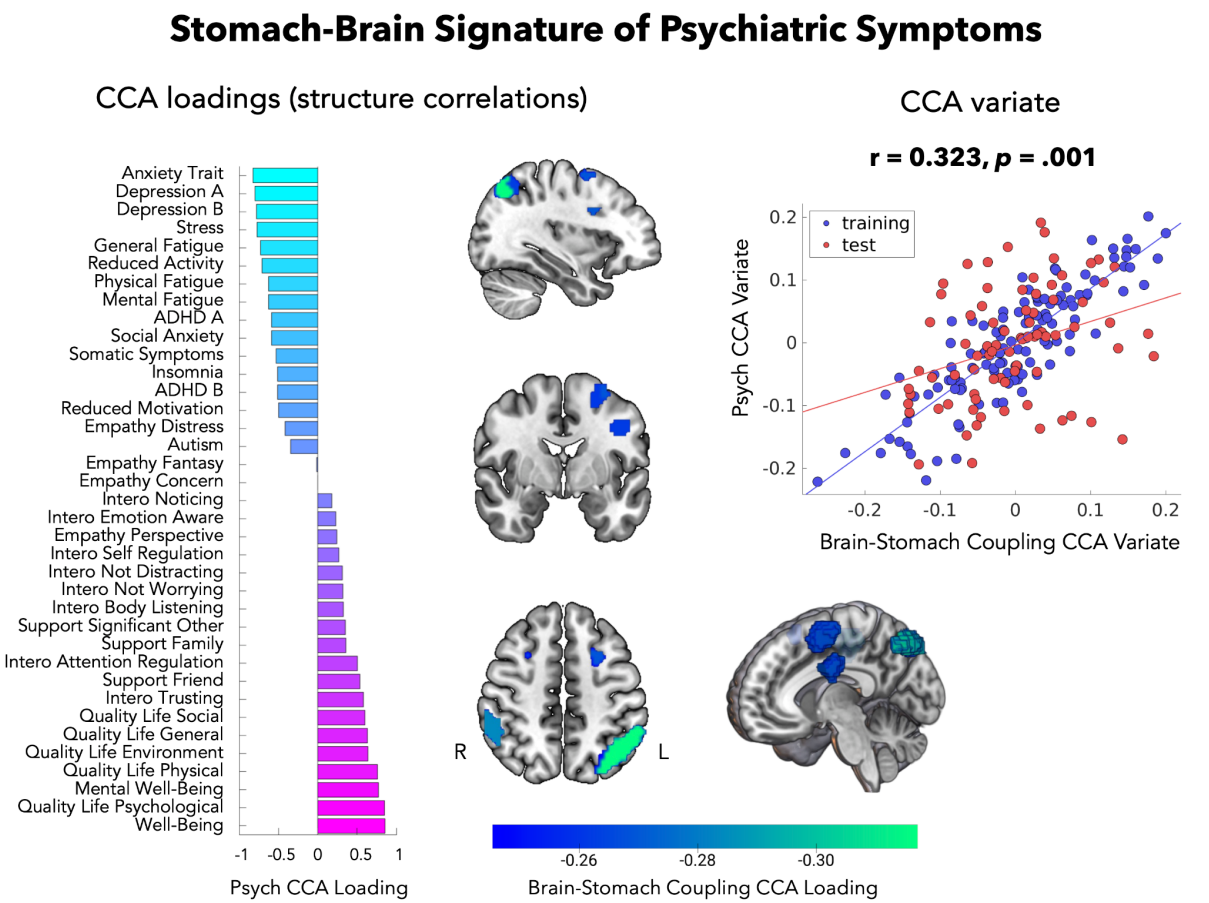

***Figure 2*: Psychiatric functional correlate of stomach-brain coupling.**

Canonical Correlation Analysis results depicting the correlation between stomach-brain coupling and psychopathology symptoms. Left panel depicts the CCA loadings (structure correlations: Pearson's correlations between raw psychiatric and stomach-brain coupling variables and their respective canonical variate). Importantly, this represents the pattern of psychiatric data that is maximally correlated with the stomach-brain coupling canonical variate. High negative loadings are shown for anxiety, depression, stress, fatigue, ADHD, somatic symptoms, and insomnia, while high positive loadings are shown for well-being and quality of life. The middle panel shows the top 5 DiFuMo parcellated regions with the absolute highest stomach-brain coupling loadings (all negative), coloured according to their respective CCA loading: left superior angular gyrus, right posterior supramarginal gyrus, left inferior precentral sulcus, left posterior superior frontal gyrus and left posterior intraparietal sulcus (plotted on a standard mni152 brain template using MRIcroGL: MNI coordinates: -34, -3, 48). Right depicts the cross-validated CCA result denoting the maximally correlated psychiatric variate and brain-stomach coupling variate (in-sample $r(118) = 0.886$, out-sample $r(77) = 0.323$, $p = 0.001$).

To further summarise our findings, we averaged parcel-level stomach-brain canonical loadings across the Yeo 7-networks[33], and also averaged psychiatric canonical loadings across the mental health categories indicated in Figure 2. This revealed the highest absolute network level stomach brain loadings in the dorsal attention (-0.132), frontoparietal control (-0.100), and ventral attention salience network (-0.061). This pattern of stomach-brain coupling was maximally correlated with the corresponding averaged psychiatric structure, in particular with strong negative loadings for depression (-0.791), stress (-0.773), anxiety (-0.709), and fatigue (-0.642), and strong positive loadings for well-being (0.815) and quality of life (0.696) (see Figure 3, and Supplementary Figure 4 for an averaged summary of the raw weights).

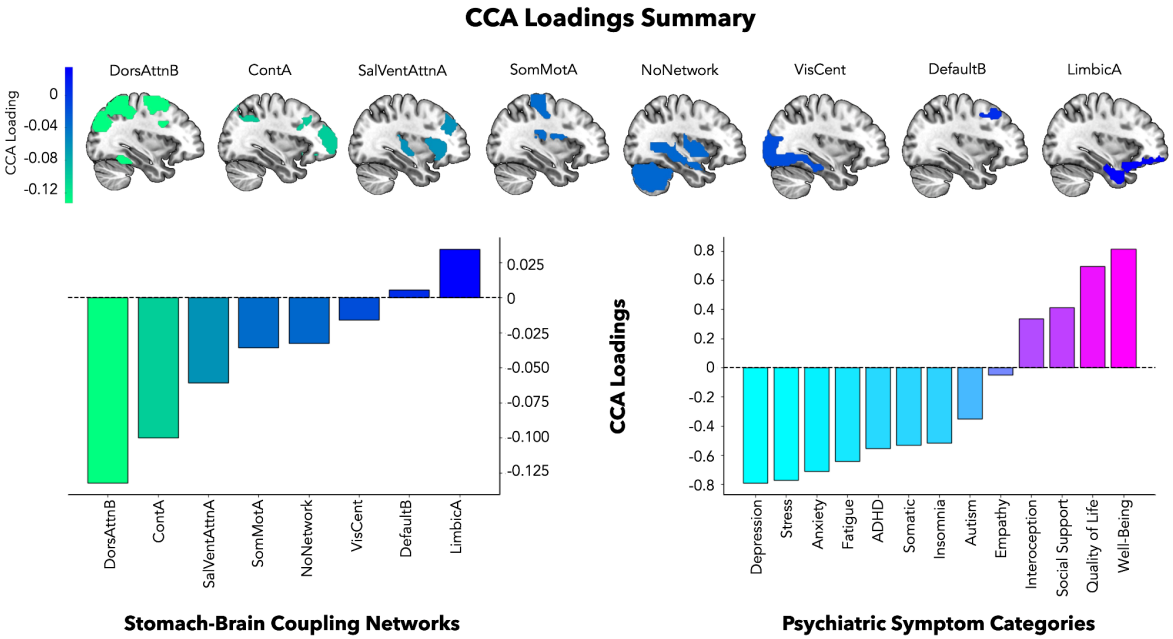

***Figure 3*: CCA loadings averaged summary.**

Canonical loadings (structure correlations: Pearson's correlations between raw inputted variables and respective canonical variate) from the psychiatric stomach-brain coupling CCA, summarised via averaging. Left shows the stomach-brain loadings averaged according to yeo-7 networks. Above demonstrates these network-averaged stomach-brain loadings projected onto a mask of the DiFuMo regions for each yeo-7 network (from left to right: DorsAttnB = Dorsal Attention B, ContA = Control A, SalVentAttnA = Salience Ventral Attention A, SomMotA = Somatomotor A, NoNetwork = no network found, VisCent = Visual A, DefaultB = Default Mode B, LimbicA = Limbic A)[33], plotted on a standard mni152 brain template using MRIcroGL: MNI coordinates: -34, -3, 48. Right illustrates the psychiatric loadings averaged across psychiatric symptom categories defined for visualisation in Figure 1.

CCA control analyses

To evaluate the specificity and robustness of these results, we conducted control CCAs predicting mental health scores from either 1) functional connectivity or 2) BOLD signal variability instead of from stomach-brain coupling. In both cases no significant canonical variate was found ($p > 0.05$, Bonferonni threshold = 0.01), indicating that the observed canonical correlations linking the gastric brain to mental health symptoms are unlikely to be explained by residual BOLD connectivity or signal variability.

We conducted a further control analysis to determine if a simpler univariate model would yield comparable results as to our multivariate approach. Independent principal components analysis (PCA) of the psychiatric scores yielded a highly similar latent structure as that derived from the CCA ($r(35) = -0.999$, $p < .001$) (see Supplementary Figure 5). We then correlated this mental health symptom PCA component with stomach-brain coupling values from each DiFuMo parcellated region separately. This revealed significant correlations of stomach-brain coupling with the psychiatric PCA component in 9 DiFuMo parcellated regions, all of which were in the top loading regions of the CCA, with the exception of the 'lateral fissure anterior' (see Supplementary Table 4). Furthermore, across all brain regions, loadings from the stomach-brain coupling CCA were highly correlated with the univariate correlation coefficients linking mental health symptoms to stomach-brain coupling ($r(207) = -0.870$, $p < .001$) (see Supplementary Figure 5). These results complement our cross-validation procedure by demonstrating that the multivariate CCA model detected effects which could be reproduced with a simpler, albeit less sensitive, model.

EGG control analyses

To control for possible low-level physiological confounds, we further estimated the association between the psychiatric canonical variate loadings and summary electrogastrographic (EGG) metrics, using non-parametric Spearman's rank order correlation coefficient (see Supplementary Table 2 for EGG metric descriptive statistics). We did not observe a significant correlation of normogastric EGG activity measured via the proportion of normogastric power, maximum power, or peak frequency with the observed psychiatric canonical variate (smallest *FDR-corrected* $p = 0.267$). Therefore, the link between stomach-brain coupling is specific to the strength of brain-body coupling and mental health symptoms, rather than being explained by baseline differences in peripheral gastric physiology.

Discussion

Our study reveals a distinctive stomach-brain signature for psychiatric symptoms, established through cross-validated multivariate regression techniques and control analyses. This signature encapsulates a positive-to-negative latent dimension of mental health, with notable negative loadings on anxiety, depression, stress, fatigue, as well as enhanced well-being and quality of life. Significantly, all 20 of the highest loadings for stomach-brain coupling were negative, indicating a direct correlation between diminished gastric-brain coupling and improved mental health (refer to Supplementary Table 5). Our control analyses confirm that this psychiatric signature is uniquely attributable to stomach-brain coupling, distinct from factors such as residual brain connectivity or variability, gastric activity variations, and bodily mass differences.

Our main result highlights the role of gastric coupling in brain regions which are known transdiagnostic hotspots in mental health, such as the posterior superior frontal gyrus and the posterior intraparietal sulcus[34,35]. Notably, the left superior angular gyrus, our model's most prominently featured region, is crucial for its integrative role in various cognitive functions[36]. This region is also associated with a range of psychiatric disorders, including schizophrenia[37], somatization disorder[38], and major depressive disorder[39,40]. Thus, the implication of these regions reveals the role of gastric rhythms in modulating neural hubs which are highly sensitive to disruption in mental health. At a cognitive level, the brain areas in which symptoms were most significantly associated with the gastric axis comprised attentional and control network hubs[33]. This indicates that top-down attentional and inhibitory control mechanisms may be particularly important for viscerally mediated psychopathology. Beyond these control oriented networks, we also observed a negative association with the ventral salience network[42], weak negative loadings in the somatomotor network[41], and weak positive loadings in the limbic system, which are thought to play an important role in linking bottom-up visceral and somatic information to emotion and selfhood, emphasising the multidimensional nature of the signature.

This research significantly advances our understanding of the clinical importance of stomach-brain coupling[18,19,43,44]. While previous smaller scale studies have linked stomach-brain coupling with bodily shame and weight preoccupation[45], our multivariate CCA approach leverages our extensive sample

size to encompass a continuum of transdiagnostic psychiatric symptoms. Importantly, although our analyses do not focus on clinical diagnostic categories, our multivariate symptom-based approach is advantageous in directly assessing highly individualistic symptom profiles across broadly transdiagnostic dimensions, and thus accounts for the high symptom comorbidity and other issues of diagnostic categories[46–49]. Moreover, the cross-validated method we apply here is specifically optimised to estimate the continuous statistical prediction of these symptoms, while also robustly protecting against overfitting[50]. Future work could build upon these results to predict psychiatric symptoms based on stomach-brain coupling in controlled clinical samples or longitudinal studies. Additionally, the dimensional symptom-focused patterns we have identified might enhance the understanding of clustered clinical subgroups within existing diagnostic categories.

Interestingly, we identified trait anxiety as a prominent mental health symptom associated with stomach-brain coupling, but a previous study found no such relationship with state anxiety[19]. A key difference between that study and ours, was the use of a region-of-interest based approach in a smaller sample size. Our whole-brain, multivariate method was optimised to detect such effects, and likely yielded a substantial improvement in statistical power by estimating latent symptom dimensions directly. It may also be that there are distinct stomach-brain relationships with trait and state aspects of anxiety. Notably, the anxiogenic relationship of stomach-brain coupling is consistent with rodent research of increased anxiety behaviours when activating gut-innervating vagal afferents[14], as well as research with generalised anxiety disorder patients demonstrating an increased bodily reactivity and intensity of interoceptive sensations in response to adrenergic stimulation[7]. Future studies could directly modulate stomach-brain coupling using various emerging interventions as a potential means to remediate anxiety symptoms in patients[17,22,30].

One potential limitation of our study concerns our EGG data exclusion rate, which was somewhat higher than the 20% rate reported in previous EGG literature[27,51]. This increase was driven by an exhaustive quantitative and qualitative quality control protocol, which may have resulted in higher numbers of excluded participants than in previous, smaller scale studies. To assuage these concerns, we conducted additional control analyses demonstrating the validity of these procedures (see Supplementary Figure 3). Furthermore, we ensured that the excluded participants did not differ in terms of sample demographics or psychiatric symptoms, ruling out the possibility

that our quality control may have created a sampling bias which could impact our results (see Electrogastrography Methods).

Our research adds to the growing body of evidence linking a disordered gastrointestinal system to various mental health conditions[15,52,53], and it sheds new light on the frequent coexistence of gastrointestinal dysfunction with affective disorders[15]. By elucidating the multimodal interactions between the stomach and the brain in psychiatric illness, our findings lay the groundwork for novel diagnostic and therapeutic strategies targeting disordered brain-stomach interactions. This includes not only innovations like non-invasive vagus nerve stimulation, which recent studies have found to modulate stomach-brain coupling[15], but also the exploration of new mechanical[17,54] and pharmacological[22,30] interventions to remedy aberrant stomach-brain interactions. Similarly, future research could leverage newly emerging technologies such as ingestible recording devices to further elucidate the physiological mechanisms linking mental health symptoms to the stomach-brain axis[55].

In summary, our study represents the largest and most comprehensive neuroimaging sample focusing on brain body interaction to date. Our results establish the clinical relevance of stomach-brain coupling. This finding contributes significantly to multidisciplinary research on brain-body interaction and opens new avenues for therapeutic, diagnostic, and classification strategies in mental health[56].

Methods and Materials

Participants

We recruited participants as part of the Visceral Mind Project, a large brain imaging project at the Centre of Functionally Integrative Neuroscience, Aarhus University. We recorded electrogastrography (EGG) in 380 participants (230 females, 149 males, 1 other gender, median age = 24, age range = 18-56). As our aim was to apply machine learning to individual differences in psychiatric symptoms, we adopted a participant recruitment strategy that sought to maximise between subject symptom variance from fully healthy to clinically substantive severities. Accordingly, we did not explicitly exclude participants for psychiatric diagnosis, and recruited participants from a wide range of possible online communities and backgrounds. We acquired participants in two data collection cohorts by advertising on nation-wide participant pools, social media, newspapers, and posted fliers. As additional criteria, participants had

normal or corrected-to-normal vision and were fluent in Danish or English. Furthermore, we only included participants compatible with MRI scanning (not pregnant/breastfeeding, no metal implants, claustrophobia etc).

Participants took part in multiple sessions including fMRI scans, behavioural tasks, physiological recordings, and psychiatric/lifestyle inventories. In this study, we focus on resting state fMRI data, electrogastrography (EGG) recordings, and a psychiatric/lifestyle assessment battery to evaluate individual differences in gastric-brain coupling and their link to mental health and psychopathology. We compensated individuals for participating. The local Region Midtjylland Ethics Committee granted approval for the study and all participants provided informed consent. The study was conducted in accordance with the Declaration of Helsinki. After the removal of poor-quality fMRI and EGG data (see quality control below), we estimated stomach-brain-coupling in 243 participants. Including the mental health scores, a total of 199 full-dataset participants were included in the psychiatric functional correlate analysis (138 females, 61 males, median age = 23, age range = 18-47) (see Supplementary Figure 1).

Anatomical and resting state fMRI acquisition

We acquired anatomical MRI and resting state fMRI data using a 3T MRI scanner (Siemens Prisma) with a 32-channel head coil. We positioned small cushions around the head to minimise head movement. The participants wore earplugs and were instructed not to move. The resting state scan included 600 volumes acquired over 14 minutes using a T2*-weighted echo-planar imaging (EPI) multiband accelerated sequence (TR = 1400ms, TE = 29.6ms, voxel size = 1.79 x 1.79 x 1.80 mm). An acceleration factor of 4 was used in the slice direction along with GRAPPA in-plane acceleration factor = 2. A set of high-resolution whole brain T1-weighted anatomical images (0.9 mm^3 isotropic) were acquired using an MP-RAGE sequence (repetition time = 2.2s, echo time = 2.51ms, matrix size = 256 × 256 x 192 voxels, flip angle = 8°, AP acquisition direction).

Physiological recording acquisition

We simultaneously recorded physiological measurements (photoplethysmography, respiratory breathing belt, and EGG) during resting-state fMRI. For the EGG recordings, we cleaned the abdomen and applied abrasive gel to remove dead skin and improve the signal-to-noise ratio. Three electrogastrography recording montages were implemented using a Brain Vision MRI-compatible ExG system and amplifier (see Supplementary Figure 2

for each recording montage consisting of 1, 3 or 6 bipolar channels). All physiological montages were acquired with a sampling rate of 1000 Hz, a low-pass filter of 1000 Hz, and no high-pass filter (DC recordings). EGG was recorded at a 0.5 μV/bit resolution, and +/- 16.384 mV range, while photoplethysmography and respiratory recordings were acquired at 152.6 μV/bit resolution, and +/- 5000 mV range.

MRI and fMRI preprocessing

We implemented the minimal preprocessing pipeline in fmriprep. MRI and fMRI results included in this manuscript come from preprocessing performed using fMRIPrep 22.1.1, which is based on Nipype 1.8.5 (see Supplementary Material for anatomical and functional MRI preprocessing details with fMRIPrep). Additional fMRI preprocessing steps following fMRIPrep included spatial smoothing with a 3mm FWHM kernel, and regressing out six motion parameters, six aCompCor parameters, as well as 13 RETROICOR components reflecting cardiac and respiratory physiological noise.

Electrogastrography peak selection and preprocessing

The EGG data was first demeaned and downsampled from 1000 Hz to 10 Hz, followed by computing the power spectrum using a Hanning-tapered fast Fourier transform (FFT) incorporating 1000 seconds of zero-padding in 200-second data segments with 75% overlap. For each participant, we selected the bipolar EGG channel that showed the most prominent peak within the normogastric range (0.033-0.066 Hz). Specifically, two researchers (L.B. and I.R.) independently conducted peak selection by visually inspecting each channel to identify the EGG channel with the highest normogastric power peak, without large artefacts and with power above 5 μv^2. Peak quality was rated as 'excellent' for gaussian-like peaks (n=184) and 'good' for shoulder-like peaks (n=81); those not meeting these standards were deemed 'poor quality' (n=115) and excluded. This visual inspection approach is consistent with previous research to account for noise in the normogastric window, or cases of multiple peaks[18,19,27].

As an additional check, we computed signal quality metrics using a comparison template-based procedure of 10 ideal participants with very clear and prominent gastric peaks. ‘Poor quality’ participants had significantly lower signal quality as measured by cosine similarity (excellent/good quality: Median = 0.963, Range = 0.667, poor quality: Median = 0.595, Range = 0.585; U = 63780, $p <$ .001, r_{rb} = 3.186) and Pearson’s correlation (excellent/good quality: Median = 0.950, Range = 1.169, poor quality: Median = 0.054, Range = 1.287; U = 63849, p < 0.001, r_{rb} = 3.190) (see Supplementary Figure 3). As an extra precaution, we

confirmed that the psychiatric scores of the included and excluded EGG participants did not significantly differ when using the first PCA component of the 37 psychiatric scores (excellent/good quality: Median = 3.766, Range = 150.429, poor quality: Median = 5.745, Range = 106.762; U = 46989, p = 0.964, r_{rb} = 2.084). The selected EGG channel was then bandpass filtered, centred at the individual peak frequency (filter width of ±0.015 Hz, filter order of 5 or 1470 samples). After phase correction, the data was resampled to the fMRI rate (0.7143 Hz) and processed through a Hilbert transform to calculate the average phase per volume.

Gastric-brain coupling estimation

We followed procedures validated in previous EGG studies to estimate gastric-brain coupling[18,19]. Briefly, BOLD time series of all brain voxels were bandpass filtered with the same filter parameters as the ones used for the EGG preprocessing. The initial and final 21 volumes (29.4 seconds) were discarded from both the BOLD and EGG time series. The updated duration of the fMRI and EGG signals in which the rest of the analysis was performed was 781.2 seconds. The Hilbert transform was applied to the BOLD and EGG time series to derive the instantaneous phases of the signals. The phase-locking value (PLV) was computed as the absolute value of the time average difference in the angle between the phases of the EGG and each voxel across time (see Equation 1). The PLV is quantified by values ranging from 0 (representing a total absence of phase synchrony) to 1 (corresponding to absolute phase synchrony).

$$PLV_{x,y} = \left| \frac{1}{T} \sum_{t=1}^{T} e^{i(\varphi x(t) - \varphi y(t))} \right|$$

Equation 1: where T is the number of time samples, and x and y are brain and gastric time series.

In order to account for any biases in PLV that arise from differences in signal amplitude, we created surrogate PLV values by disrupting the phase relationship between EGG and BOLD time series. We achieved this by shifting the EGG by at least ±60 s with respect to the BOLD time series, with concatenation at the edges. Given the 558 samples in the BOLD time series, this procedure generated 472 surrogate PLV datasets. We then took the median value of these surrogate PLV distributions as chance level coupling, and defined coupling strength as the difference between empirical and chance level

coupling. Therefore, a higher value represents stronger stomach-brain coupling strength.

Psychiatric symptom assessment battery

Participants completed a battery of psychiatric and lifestyle assessments. This encompassed 16 separate survey instruments spanning autism, ADHD, empathy, insomnia, interoception, depression, fatigue, social support, somatic symptoms, stress, social anxiety, trait anxiety, well-being, and quality of life. All scales utilised validated Danish translations, except in cases where participants spoke English as their first language, in which case validated English versions were used. This allowed us to explore a broad range of psychiatric symptoms and lifestyle factors across 37 subscale scores (see Supplementary Table 1 for details of surveys, abbreviations, and subscale scores).

Canonical correlation analysis

We used the CCA-PLS toolbox to fit multivariate, cross-validated Canonical Correlation Analysis (CCA) models relating stomach-brain coupling (coupling strength of the BOLD and EGG time series) to psychiatric symptom scores. Specifically, CCA aims to find linear combinations of each multidimensional variable (i.e., canonical variates: which are weighted sums of stomach-brain coupling ($V = X * B$) and mental health ($U = Y * A$)) that are maximally correlated with each other, but uncorrelated with all other combinations (X and Y represent the inputted stomach-brain coupling and mental health data, while A and B represent the canonical weights)[50,57]. The toolbox incorporates various CCA/PLS models, including the cross-validated and optimised PCA-CCA techniques applied here[50].

We first reduced the dimensions of stomach-brain coupling per fMRI voxel by parcellating with the 256-region Dictionary of Functional Modes (DiFuMo) atlas, excluding regions of cerebrospinal fluid, ventricles, or white matter, yielding 209 relevant regions. Because CCA can be sensitive to outliers[58], participants were then screened for outliers in stomach-brain coupling and psychiatric data, leading to the exclusion of 12 and 25 participants, respectively (see Supplementary Figure 1 for a complete flow chart of exclusions). Our final Canonical Correlation Analysis (CCA) sample comprised 199 participants for whom we had complete stomach-brain coupling and psychiatric symptom matrices. These were standardised to have zero mean and unit variance, and nuisance regression was applied to control the estimated canonical variates for the influence of gender, age, body mass index, and data collection cohort.

Subsequently, we applied the cross-validated CCA approach within the predictive framework (machine learning) provided by the CCA-PLS toolbox[50]. This predictive approach involved randomly splitting the data into a training/optimisation set (60% of the overall data) and a test/holdout set (40% of the overall data) 5 times (5-fold cross-validation). These optimisation and holdout sets are known as the 'outer data splits', used for statistical inference (determining the number of significant associative CCA modes). The p-values were calculated via permutation testing (1000 permutations), as the fraction of the shuffled permuted out-of-sample correlations exceeding the out-of-sample correlation in the non-permuted holdout set. Because we implemented 5 holdout sets, the p-value for each holdout set was Bonferroni corrected (a = 0.05/5 = 0.01). An associative CCA effect is considered significant if the p-value was significant in at least one of the independent test/holdout sets, once trained on the training/optimisation set (out-of-sample correlation). If a significant associative CCA effect was found, the CCA iteratively removed the effect from the data via deflation and repeated this approach to find orthogonal CCA associative effects.

Before statistical inference, to overcome multicollinearity and overfitting issues, the PCA-CCA approach optimises the number of features (PCA components) inputted to each of the outer data splits used for statistical inference. Thus, the PCA-CCA approach further divides the optimisation set into a training set (60% of the optimisation set) and a validation set (40% of the optimisation set) 5 times (5-fold hyperparameter optimisation) for each outer data split. These 'inner data splits' were used to select the optimal hyperparameters (number of PCA components the inputted stomach-brain coupling and psychiatric data dimensions were reduced to) by maximising the average out-of-sample correlation in the validation sets.

To aid interpretation of the networks underlying the estimated brain-stomach coupling signature, we visualised overall network-level contributions by averaging the canonical loadings across the Yeo 7-network parcellation for the stomach-brain coupling axis[33]. Moreover, we averaged across psychiatric symptom categories for the psychiatric loading axis (see Figure 3).

Control analyses

To control for underlying influences of neural connectivity or brain activity variability to the psychiatric stomach-brain coupling result, we conducted two separate control CCA analyses. For the neural connectivity control analysis, we parcellated the fMRI preprocessed data (with an additional high-pass filter to handle low-frequency signal drifts) with the same method used for the stomach-

brain coupling data (using the 256-DiFuMo atlas and removing cerebrospinal fluid, ventricles, and white matter regions), and quantified individual functional connectivity data matrices using correlation (Nilearn function: 'ConnectivityMeasure.fit_transform'). Furthermore, for the brain activity variability control analysis, we calculated the standard deviation of BOLD activity for each voxel of the fMRI preprocessed data and parcellated using the same method. Both the resting connectivity and BOLD signal variability control CCA analyses were completed with the same CCA parameters as described in the methods section of the manuscript.

As an additional control, we conducted a separate whole brain analysis to determine if we could identify a similar result when using a simpler mass univariate analysis. First, we computed PCA on the psychiatric scores to get a single mental health component similar to the psychiatric canonical loadings from the CCA. This independent psychiatric PCA component was then correlated with the stomach-brain coupling from each of the 209 DiFuMo parcellated regions separately. Finally, these univariate Pearson correlation coefficients were correlated with the stomach-brain coupling loadings from the multivariate CCA to determine similarity of the two analysis strategies.

Moreover, we completed control Spearman correlations of gastric physiology (EGG metrics) with the psychiatric canonical variate extracted from the stomach-brain coupling CCA analysis. From the computed EGG power spectra (as described in the electrogastrography preprocessing section), we quantified the following normogastric EGG metrics: peak frequency, maximum power, and proportion of power (see Supplementary Table 2). Specifically, within the normogastric frequency range (0.033-0.067 Hz/2-4 cpm/15-30 seconds), we stored the peak frequency and maximum power. Furthermore, we computed the proportion of normogastric power as the sum of the normogastric power divided by the sum of the power in all gastric frequencies (including bradygastric, normogastric, and tachygastric frequencies: 0.02-0.17 Hz/1-10 cpm/6-60 seconds). We input those EGG metrics into a correlation matrix with the psychiatric canonical variate, correcting for multiple comparisons using the false-discovery rate (FDR) at 5%.

Acknowledgements

This research is financially supported by a Lundbeckfonden Fellowship (R272-2017-4345) and a European Research Council Grant (ERC-2020-StG-948788). IR was supported by the Marie Skłodowska-Curie Action (MSCA) BRAINSTOM (grant agreement No 101028203). The funding sources were not involved in the study design, collection, analysis, interpretation, or writing of the manuscript.

LB and IR analysed the data, interpreted the results, and wrote the manuscript, NN provided conceptual advice and contributed towards preprocessing of neuroimaging data, MA provided supervision, conceptual advice, and wrote the manuscript.

Deidentified participant data and scripts implemented in this paper are available here: https://github.com/embodied-computation-group/StomachBrain-MentalHealth

Disclosures

All authors declare no conflicts of interest.

References

1. Gallagher, S. Philosophical conceptions of the self: implications for cognitive science. *Trends Cogn. Sci.* **4**, 14–21 (2000).
2. Engelen, T., Solcà, M. & Tallon-Baudry, C. Interoceptive rhythms in the brain. *Nat. Neurosci.* **26**, 1670–1684 (2023).
3. Allen, M. Unravelling the Neurobiology of Interoceptive Inference. *Trends Cogn. Sci.* (2020) doi:10.1016/j.tics.2020.02.002.
4. Critchley, H. D. & Garfinkel, S. N. Interoception and emotion. *Curr. Opin. Psychol.* **17**, 7–14 (2017).
5. Nord, C. L. & Garfinkel, S. N. Interoceptive pathways to understand and treat mental health conditions. *Trends Cogn. Sci.* **26**, 499–513 (2022).
6. Hsueh, B. *et al.* Cardiogenic control of affective behavioural state. *Nature* **615**, 292–299 (2023).
7. Teed, A. R. *et al.* Association of Generalized Anxiety Disorder With Autonomic Hypersensitivity and Blunted Ventromedial Prefrontal Cortex Activity During Peripheral Adrenergic Stimulation: A Randomized Clinical Trial. *JAMA Psychiatry* **79**, 323–332 (2022).
8. Cryan, J. F. & Dinan, T. G. Mind-altering microorganisms: the impact of the gut microbiota on brain and behaviour. *Nat. Rev. Neurosci.* **13**, 701–712 (2012).
9. Kolobaric, A. *et al.* Gut microbiome predicts cognitive function and depressive symptoms in late life. *Mol. Psychiatry* 1–12 (2024) doi:10.1038/s41380-024-02551-3.
10. Allen, M., Varga, S. & Heck, D. H. Respiratory rhythms of the predictive mind. *Psychol. Rev.* (2022).
11. Bagur, S. *et al.* Breathing-driven prefrontal oscillations regulate maintenance of conditioned-fear evoked freezing independently of initiation. *Nat. Commun.* **12**, 2605 (2021).
12. Kluger, D. S. *et al.* Modulatory dynamics of periodic and aperiodic activity in respiration-brain coupling. *Nat. Commun.* **14**, 4699 (2023).
13. Zelano, C. *et al.* Nasal Respiration Entrains Human Limbic Oscillations and Modulates Cognitive Function. *J. Neurosci.* **36**, 12448–12467 (2016).
14. Krieger, J.-P. *et al.* Neural Pathway for Gut Feelings: Vagal Interoceptive Feedback From the Gastrointestinal Tract Is a Critical Modulator of Anxiety-like Behavior. *Biol. Psychiatry* **92**, 709–721 (2022).
15. Margolis, K. G., Cryan, J. F. & Mayer, E. A. The Microbiota-Gut-Brain Axis: From Motility to Mood. *Gastroenterology* **160**, 1486–1501 (2021).
16. Foster, J. A. & McVey Neufeld, K.-A. Gut–brain axis: how the microbiome influences anxiety and depression. *Trends Neurosci.* **36**, 305–312 (2013).
17. Mayeli, A. *et al.* Parieto-occipital ERP indicators of gut mechanosensation in humans. *Nat. Commun.* **14**, 3398 (2023).
18. Rebollo, I., Devauchelle, A.-D., Béranger, B. & Tallon-Baudry, C. Stomach-brain synchrony reveals a novel, delayed-connectivity resting-state network in humans. *eLife* **7**, e33321 (2018).

19. Rebollo, I. & Tallon-Baudry, C. The sensory and motor components of the cortical hierarchy are coupled to the rhythm of the stomach during rest. *J. Neurosci.* **42**, 2202–2220 (2021).
20. Azzalini, D., Rebollo, I. & Tallon-Baudry, C. Visceral Signals Shape Brain Dynamics and Cognition. *Trends Cogn. Sci.* **23**, 488–509 (2019).
21. Teckentrup, V. & Kroemer, N. B. Mechanisms for survival: vagal control of goal-directed behavior. *Trends Cogn. Sci.* **28**, 237–251 (2024).
22. Nord, C. L., Dalmaijer, E. S., Armstrong, T., Baker, K. & Dalgleish, T. A Causal Role for Gastric Rhythm in Human Disgust Avoidance. *Curr. Biol.* **31**, 629-634.e3 (2021).
23. Inui, A. Ghrelin: An orexigenic and somatotrophic signal from the stomach. *Nat. Rev. Neurosci.* **2**, 551–560 (2001).
24. Sanders, K. M., Ward, S. M. & Koh, S. D. Interstitial Cells: Regulators of Smooth Muscle Function. *Physiol. Rev.* **94**, 859–907 (2014).
25. Richter, C. G., Babo-Rebelo, M., Schwartz, D. & Tallon-Baudry, C. Phase-amplitude coupling at the organism level: The amplitude of spontaneous alpha rhythm fluctuations varies with the phase of the infra-slow gastric basal rhythm. *NeuroImage* **146**, 951–958 (2017).
26. Cao, J. *et al.* Gastric stimulation drives fast BOLD responses of neural origin. *NeuroImage* **197**, 200–211 (2019).
27. Müller, S. J., Teckentrup, V., Rebollo, I., Hallschmid, M. & Kroemer, N. B. Vagus nerve stimulation increases stomach-brain coupling via a vagal afferent pathway. *Brain Stimulat.* **15**, 1279–1289 (2022).
28. Cao, J., Wang, X., Chen, J., Zhang, N. & Liu, Z. The vagus nerve mediates the stomach-brain coherence in rats. *NeuroImage* **263**, 119628 (2022).
29. Marso Steven P. *et al.* Semaglutide and Cardiovascular Outcomes in Patients with Type 2 Diabetes. *N. Engl. J. Med.* **375**, 1834–1844 (2016).
30. Wilding John P.H. *et al.* Once-Weekly Semaglutide in Adults with Overweight or Obesity. *N. Engl. J. Med.* **384**, 989–1002 (2021).
31. Nummenmaa, L., Glerean, E., Hari, R. & Hietanen, J. K. Bodily maps of emotions. *Proc. Natl. Acad. Sci.* **111**, 646–651 (2014).
32. Lachaux, J.-P., Rodriguez, E., Martinerie, J. & Varela, F. J. Measuring phase synchrony in brain signals. *Hum. Brain Mapp.* **8**, 194–208 (1999).
33. Yeo, B. T. T. *et al.* The organization of the human cerebral cortex estimated by intrinsic functional connectivity. *J. Neurophysiol.* **106**, 1125–1165 (2011).
34. McTeague, L. M. *et al.* Identification of Common Neural Circuit Disruptions in Cognitive Control Across Psychiatric Disorders. *Am. J. Psychiatry* **174**, 676–685 (2017).
35. Yang, Y. *et al.* Common and Specific Functional Activity Features in Schizophrenia, Major Depressive Disorder, and Bipolar Disorder. *Front. Psychiatry* **10**, (2019).
36. Seghier, M. L. The Angular Gyrus. *The Neuroscientist* **19**, 43–61 (2013).
37. Gao, Y. *et al.* Decreased resting-state neural signal in the left angular gyrus as a

potential neuroimaging biomarker of schizophrenia: An amplitude of low-frequency fluctuation and support vector machine analysis. *Front. Psychiatry* **13**, (2022).

38. Su, Q. *et al.* Decreased interhemispheric functional connectivity in insula and angular gyrus/supramarginal gyrus: Significant findings in first-episode, drug-naive somatization disorder. *Psychiatry Res. Neuroimaging* **248**, 48–54 (2016).
39. Gao, J. *et al.* Habenula and left angular gyrus circuit contributes to response of electroconvulsive therapy in major depressive disorder. *Brain Imaging Behav.* **15**, 2246–2253 (2021).
40. Mo, Y. *et al.* Bifrontal electroconvulsive therapy changed regional homogeneity and functional connectivity of left angular gyrus in major depressive disorder. *Psychiatry Res.* **294**, 113461 (2020).
41. Gordon, E. M. *et al.* A somato-cognitive action network alternates with effector regions in motor cortex. *Nature* **617**, 351–359 (2023).
42. Menon, V. & Uddin, L. Q. Saliency, switching, attention and control: a network model of insula function. *Brain Struct. Funct.* **214**, 655–667 (2010).
43. Choe, A. S. *et al.* Phase-locking of resting-state brain networks with the gastric basal electrical rhythm. *PLOS ONE* **16**, e0244756 (2021).
44. Levakov, G., Ganor, S. & Avidan, G. Reliability and validity of brain-gastric phase synchronization. *Hum. Brain Mapp.* **44**, 4956–4966 (2023).
45. Todd, J., Cardellicchio, P., Swami, V., Cardini, F. & Aspell, J. E. Weaker implicit interoception is associated with more negative body image: Evidence from gastric-alpha phase amplitude coupling and the heartbeat evoked potential. *Cortex* **143**, 254–266 (2021).
46. Krueger, R. F. *et al.* Progress in achieving quantitative classification of psychopathology. *World Psychiatry* **17**, 282–293 (2018).
47. Regier, D. A. *et al.* DSM-5 Field Trials in the United States and Canada, Part II: Test-Retest Reliability of Selected Categorical Diagnoses. *Am. J. Psychiatry* **170**, 59–70 (2013).
48. Kotov, R. *et al.* The Hierarchical Taxonomy of Psychopathology (HiTOP): A dimensional alternative to traditional nosologies. *J. Abnorm. Psychol.* **126**, 454–477 (2017).
49. Dalgleish, T., Black, M., Johnston, D. & Bevan, A. Transdiagnostic approaches to mental health problems: Current status and future directions. *J. Consult. Clin. Psychol.* **88**, 179–195 (2020).
50. Mihalik, A. *et al.* Canonical Correlation Analysis and Partial Least Squares for Identifying Brain–Behavior Associations: A Tutorial and a Comparative Study. *Biol. Psychiatry Cogn. Neurosci. Neuroimaging* **7**, 1055–1067 (2022).
51. Wolpert, N., Rebollo, I. & Tallon-Baudry, C. Electrogastrography for psychophysiological research: Practical considerations, analysis pipeline, and normative data in a large sample. *Psychophysiology* **57**, e13599 (2020).
52. Chang, L., Wei, Y. & Hashimoto, K. Brain–gut–microbiota axis in depression: A historical overview and future directions. *Brain Res. Bull.* **182**, 44–56 (2022).

53. Vindegaard, N., Speyer, H., Nordentoft, M., Rasmussen, S. & Benros, M. E. Gut microbial changes of patients with psychotic and affective disorders: A systematic review. *Schizophr. Res.* **234**, 41–50 (2021).
54. Rao, S. S. C., Quigley, E. M. M., Chey, W. D., Sharma, A. & Lembo, A. J. Randomized Placebo-Controlled Phase 3 Trial of Vibrating Capsule for Chronic Constipation. *Gastroenterology* **164**, 1202-1210.e6 (2023).
55. Porciello, G., Monti, A., Panasiti, M. S. & Aglioti, S. M. Ingestible pills reveal gastric correlates of emotions. *eLife* **13**, e85567 (2024).
56. Davis, S. Tracing somatic therapies. *Lancet Psychiatry* **8**, 282–284 (2021).
57. Linke, J. O. *et al.* Shared and Anxiety-Specific Pediatric Psychopathology Dimensions Manifest Distributed Neural Correlates. *Biol. Psychiatry* **89**, 579–587 (2021).
58. Luo, L., Wang, W., Bao, S., Peng, X. & Peng, Y. Robust and sparse canonical correlation analysis for fault detection and diagnosis using training data with outliers. *Expert Syst. Appl.* **236**, 121434 (2024).

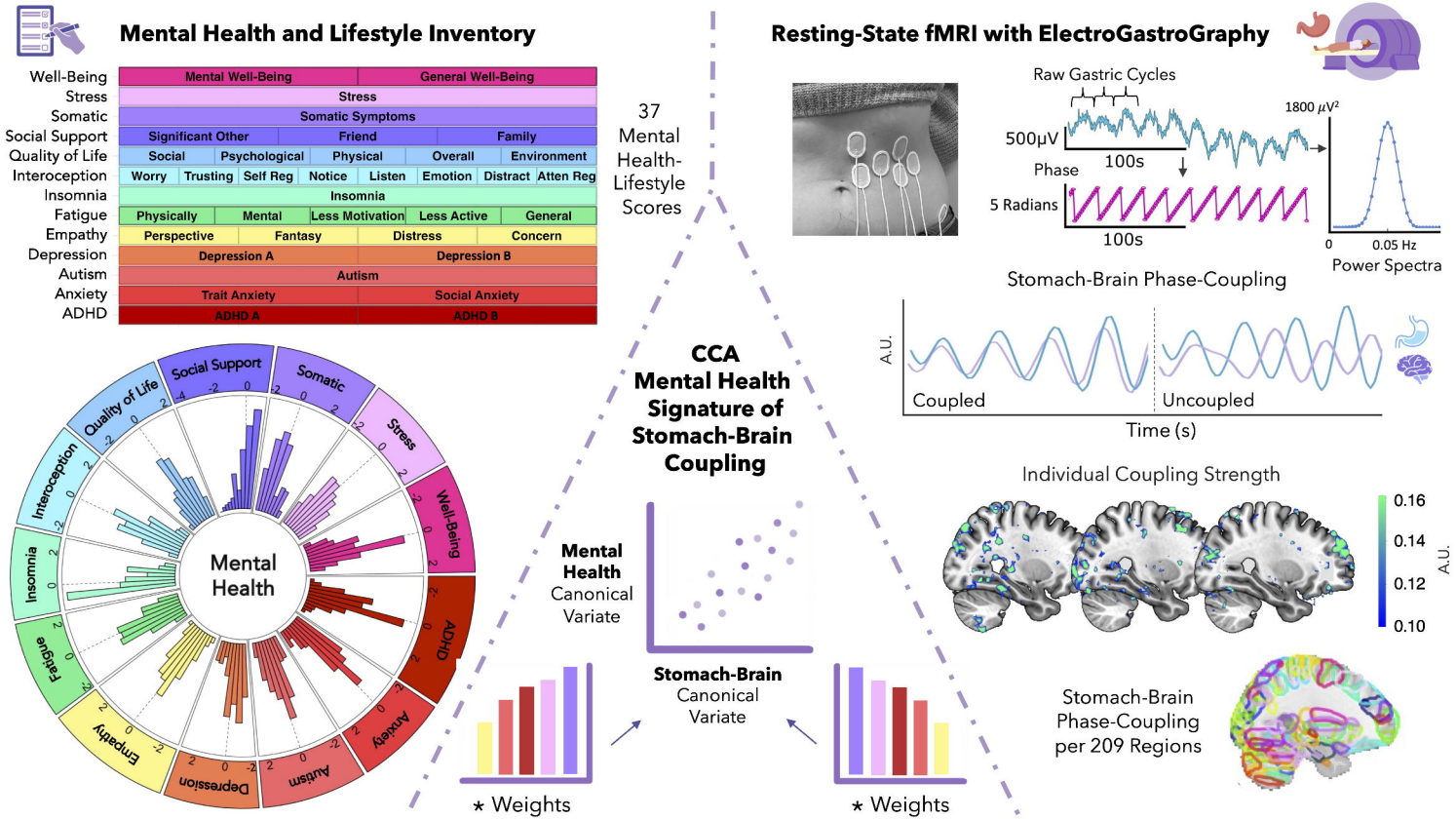
Mental Health and Lifestyle Inventory
Well-Being
Stress
Somatic
Social Support
Quality of Life
Interoception
Insomnia
Fatigue
Empathy
Depression
Autism
Anxiety
ADHD
Mental Well-Being
General Well-Being
Stress
Somatic Symptoms
Significant Other
Friend
Family
Social
Psychological
Physical
Overall
Environment
Worry
Trusting
Self Reg
Notice
Listen
Emotion
Distract
Atten Reg
Insomnia
Physically
Mental
Less Motivation
Less Active
General
Perspective
Fantasy
Distress
Concern
Depression A
Depression B
Autism
Trait Anxiety
Social Anxiety
ADHD A
ADHD B
37 Mental Health-Lifestyle Scores
Mental Health
CCA Mental Health Signature of Stomach-Brain Coupling
Mental Health Canonical Variate
Stomach-Brain Canonical Variate
* Weights
* Weights
Resting-State fMRI with ElectroGastroGraphy
Raw Gastric Cycles
500μV
100s
Phase
5 Radians
100s
1800 μV²
0
0.05 Hz
Power Spectra
Stomach-Brain Phase-Coupling
A.U.
Coupled
Uncoupled
Time (s)
Individual Coupling Strength
0.16
0.14
0.12
0.10
A.U.
Stomach-Brain Phase-Coupling per 209 Regions

Mental Health Signature of Stomach-Brain Coupling

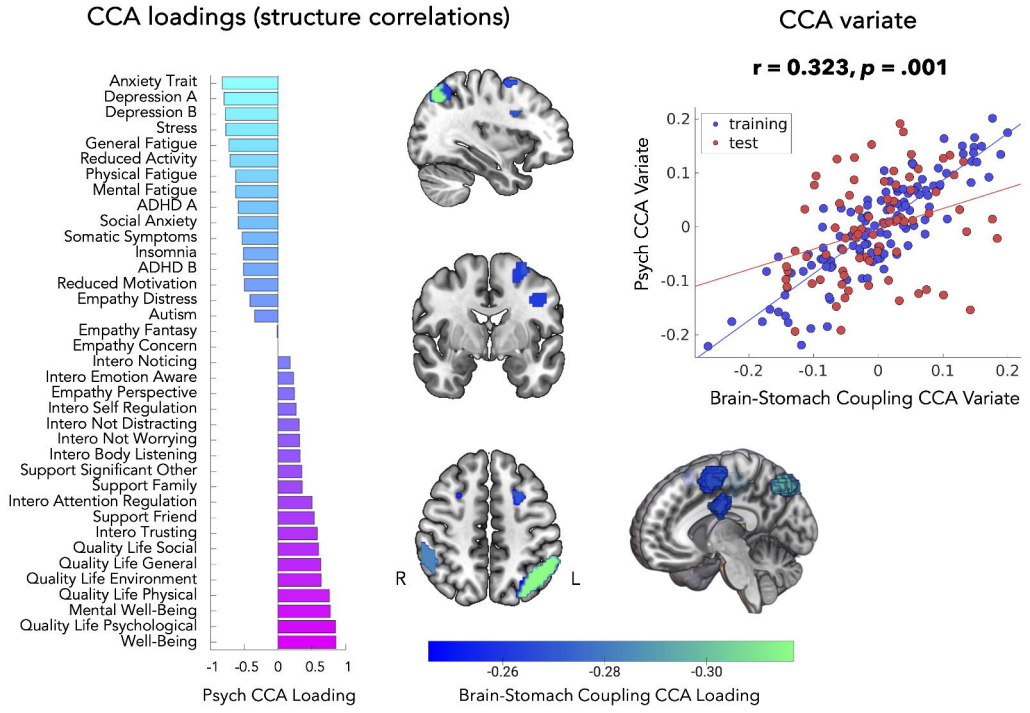

CCA Loadings Summary

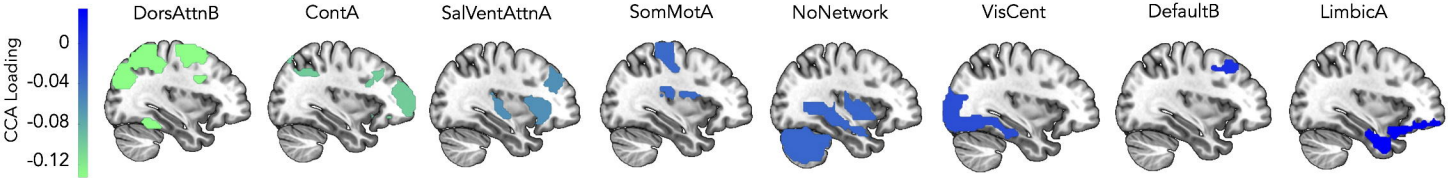

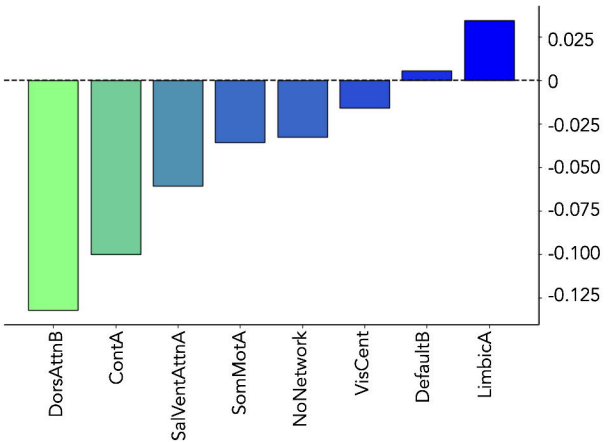

Stomach-Brain Coupling Networks

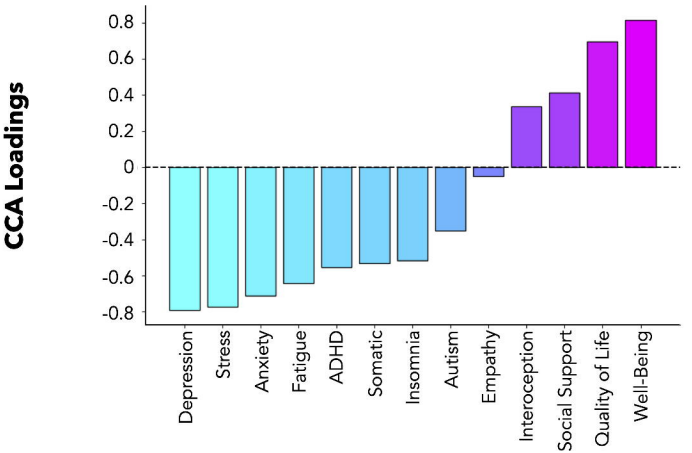

Mental Health Categories

$$PLV_{x,y} = \left| \frac{1}{T} \sum_{t=1}^{T} e^{i(\varphi x(t) - \varphi y(t))} \right|$$